Available online at www.sciencedirect.com
SCIENCE DIRECT
International Journal of Heat and Mass Transfer 49 (2006) 1299–1309
International Journal of HEAT and MASS TRANSFER
www.elsevier.com/locate/ijhmt

Modeling capability of R134a for a critical heat flux of water in a vertical 5 × 5 rod bundle geometry

Syed Waseem Akhtar [a,b], Sang-Ki Moon [a], Se-Young Chun [a,*], Sung-Deok Hong [a], Won-Pil Baek [a]

[a] Korea Atomic Energy Research Institute, Thermal Hydraulic Safety Research Department, 150, Deokjin-dong, Yuseong-gu, Daejeon 305-353, Republic of Korea
[b] Institute for Nuclear Power, P.O. Box 3140, Islamabad, Pakistan

Received 14 August 2005; received in revised form 7 October 2005
Available online 10 January 2006

Abstract

Critical heat flux (CHF) tests have been performed for a vertically upward R134a flow in a 5 × 5 rod bundle in the following parameter ranges: outlet pressure 1.5–3.0 MPa, mass flux 50–2500 kg m^{-2} s^{-1}, inlet quality −0.08 to −0.75 and critical quality −0.17 to 1.58. Parametric trends of the CHF data agree well with the general understanding. Water equivalent CHF data is generated using a set of well-established modeling parameters, then compared with (a) the EPRI/Colombia University's water CHF database for similar geometry and experimental conditions and (b) commonly used CHF prediction methods. The water equivalent CHF data generated from the present tests shows a good agreement with the actual water CHF data for both Katto's and Ahmad's modeling methods when considering the differences in the detailed geometric and flow conditions. They are also predicted well by the 1995 CHF look-up table. These results indicate that R134a can be a good modeling fluid for the CHF of water in rod bundles at least in the investigated parameter ranges.

Keywords: Fluid-to-fluid modeling; Critical heat flux; Critical quality; Rod bundle; Ahmad's parameter; Katto's parameter; Boiling number

1. Introduction

Determination of the critical heat flux (CHF) in rod bundles is of overriding importance in the thermal hydraulic design and analysis of nuclear reactors and other thermal units. The CHF is the maximum heat flux beyond which a boiling crisis occurs resulting in a sharp rise in the rod surface temperature, which may lead to a rod failure. Because of the unique hydrodynamic characteristics involved in bundle geometries, an actual experimental CHF database is extremely necessary to avoid an excessive conservatism or uncertainties in CHF estimations. However, water CHF experiments with rod bundles at the representative high-temperature and high-pressure conditions (typical of water-cooled nuclear reactors) require a large-scale facility involving a high-electrical power (due to the high latent heat and high critical pressure) as well as high testing costs, which may not be possible in an ordinary heat transfer laboratory.

As an alternative, fluid-to-fluid modeling approaches have been reported in several CHF studies [1–5]. The modeling methods reported by Ahmad [1] and Katto [2] as adopted by Groeneveld et al. [3] and subsequent researchers [4,5] are now considered as well established for modeling a CHF in circular tubes and annuli. Freons have been used very successfully for modeling a CHF of water in these studies.

Although fluid-to-fluid modeling techniques have been proved to be successful for simple geometries such as a single tube or annulus, only limited information is available for a CHF in rod bundle geometries. Furthermore, even

* Corresponding author. Tel.: +82 42 868 2948; fax: +82 42 868 8362.
E-mail address: sychun@kaeri.re.kr (S.-Y. Chun).

0017-9310/$ - see front matter © 2005 Elsevier Ltd. All rights reserved.
doi:10.1016/j.ijheatmasstransfer.2005.10.019

Nomenclature

A_f	bundle geometry flow area (m^2)
Bo	Boiling number ($= q''_{CHF}/Gh_{fg}$)
D	tube inside diameter (m)
D_{hy}	hydraulic equivalent diameter (m)
G	mass flux ($kg\,m^{-2}\,s^{-1}$)
h_{fg}	latent heat of vaporization ($kJ\,kg^{-1}$)
L	heated length (m)
P	system pressure (MPa)
q''_{CHF}	rod bundle averaged critical heat flux ($kW\,m^{-2}$)
Q_c	rod bundle total critical power (kW)
X_c	critical quality, i.e., cross-sectional averaged quality at the CHF location (–)
X_{in}	cross-sectional averaged inlet quality (–)
z	axial distance from beginning of the heated length (m)

Greek symbols

Δh_{in}	inlet subcooling enthalpy ($kJ\,kg^{-1}$)
ρ	density ($kg\,m^{-3}$)
μ	viscosity (Pa s)
σ	surface tension ($N\,m^{-1}$)
ψ	modeling parameter (–)

Subscripts

Ahmad	parameter based on Ahmad's modeling method
CHF	critical heat flux
CU data	EPRI/Columbia University's water CHF data
F	modeling fluids (Freons)
Katto	parameter based on Katto's modeling method
l	liquid
meas	measured value
pred	predicted value
pres	present (R134a or water-equivalent)
v	vapor
W	water

for simple geometries, the use of modeling techniques beyond their demonstrated range of validity (mainly subcooled or low quality and high flow conditions) can result in large errors in the CHF predictions [6]. On the other hand, it is also well known that the commonly used prediction methods, when based on a simple geometry only, are not accurately valid for rod bundles where the flow condition is additionally influenced by the bundle-specific effects (inter-channel mixing, effects due to the spacer grid and cold-wall) [7]. From this point of view, the validity of the available CHF modeling methods needs to be comprehensively assessed for rod bundle geometries. Katsaounis [8] examined the validity of the fluid-to-fluid modeling for a CHF in rod bundles under the conditions of a pressure from 1.1 to 3.7 MPa, mass flux from 600 to $3600\,kg\,m^{-2}\,s^{-1}$ and an inlet quality from −0.1 to −0.6. For comparing the Freon-12 CHF data with the EPRI/Columbia University's water CHF data [9] for similar 5×5 bundle geometries, Katsaounis's results [8] showed a reasonable modeling accuracy with Ahmad's modeling parameter for a mass flux versus critical quality. However, remarkable deviations between the water and Freon were reported for lower values of Ahmad's parameter. No direct comparison was made based on the CHF data. Similar discrepancy in the validity of the fluid-to-fluid modeling at lower mass fluxes was reported by Chun et al. [10] for an uniformly heated vertical annulus using the Boiling numbers versus Ahmad's [1] and Katto's [2] modeling parameters.

The objectives of the present study are to examine the basic parametric trends and to assess the validity of the fluid-to-fluid principles based on the R134a CHF data measured with a uniformly heated rod bundle. The water-equivalent CHF data generated from the R134a CHF data is compared with the EPRI/Colombia University's water CHF database [9] for similar (5×5 and 6×6) geometries and experimental conditions using Katto's and Ahmad's modeling methods. They are also compared with the commonly used CHF correlations for rod bundles.

2. Experimental set-up

2.1. Freon test loop

The present experiments were performed in the Freon Thermal Hydraulic Test Loop at the Korea Atomic Energy Research Institute (KAERI). The test loop uses R134a as a working fluid and can be operated up to 4.50 MPa (water-equivalent pressure is 24.5 MPa). As shown in Fig. 1, the test loop mainly consists of two circulation pumps, two preheaters, two pressurizers, a test section, two condensers and two coolers. The flow rate through the test section inlet is controlled by adjustments of the pump motor speed, the flow control valve, and the bypass valve. The inlet flow rate is measured by a Coriolis-type mass flow meter. The twin pressurizers are an accumulator-type, which control the loop pressure through a bladder filled with nitrogen gas. The nitrogen gas is introduced through the bladder in order to prevent a direct contact with R134a. A pair of preheaters is used to adjust the degree of the subcooling of the fluid entering the test section. A throttling valve located at the upstream of the test section inlet is used to avoid flow fluctuations, which usually occur at low flow conditions. The boiling two-phase flow generated in the test section is condensed by the condensers and subsequently cooled by the twin coolers. A fine adjustment in the degree of subcooling

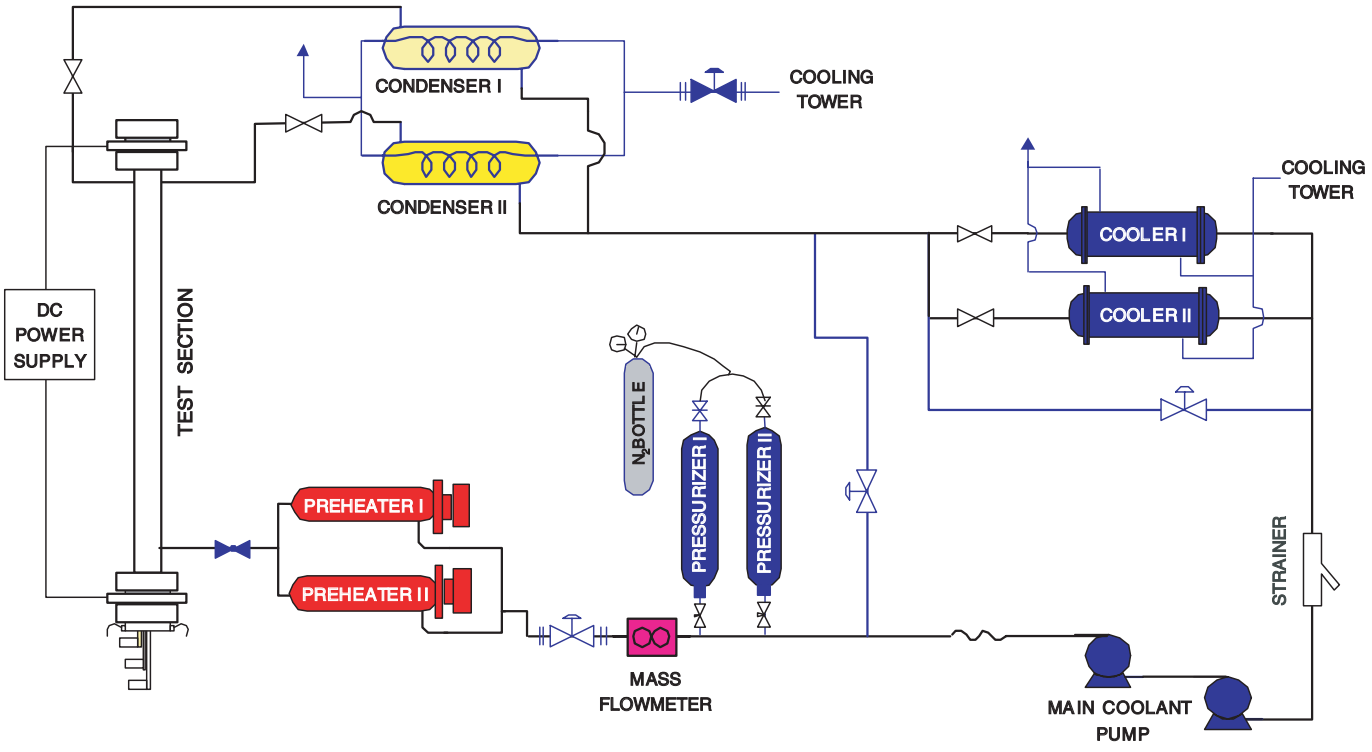

Fig. 1. Schematic diagram of the 5 × 5 Freon test loop at KAERI.

is made by a combination of adjustments in the preheater's power along with a valve opening of the heated and cooling water lines of the condensers and coolers.

2.2. Test section

The main parameters of the 5 × 5 bundle geometry are shown in Table 1 and Fig. 2. For measuring the heater rod wall temperatures for a CHF, the ungrounded K-type thermocouples with a sheath diameter of 0.5 mm were attached to the inside rod surface. These thermocouples were located at 10 mm below the top end of the vertical uniformly heated section. The radial power factor had about a 20% difference between the 9 center rods and 16 side rods. Each of the 9 center rods was instrumented with four thermocouples, while the other 16 rods contained two thermocouples. The thermocouples for each heater rod are azimuthally uniformly distributed. The heater rods were supported axially by six plain (simple support without mixing vane) spacer grids. The power to the test section is supplied from a direct current rectifier with a maximum voltage of 60 V and a maximum current of 12,000 A. An automatic power trip system is provided in the control module of the data acquisition system to protect the test section heater rods from a burnout during the CHF experiments.

Table 1
Rod bundle geometry data

Parameter	Value
Number of heated rods	25
Rod pitch (mm)	12.85
Rod diameter (mm)	9.5
Heated length (mm)	2000
Rod to wall gap (mm)	3.0
Corner radius (mm)	3.0
Flow area (mm^2)	2695.8
Hydraulic diameter (mm)	10.69
Axial power distribution	Uniform
Radial power distribution	Non-uniform
Mixing vane	No

2.3. Procedure and test matrix

The general procedure for performing CHF tests is as follows: After setting the mass flux, inlet subcooling and the exit pressure to the desired values, the power to the test section is increased gradually in small steps. At each power level, the test parameters are allowed to stabilize for several minutes to achieve a quasi-steady state condition before raising the power level again. This process is repeated until a CHF occurs, as indicated by a sharp and continuous rise in the surface temperature in any of the 25 heater rods. When the rod wall temperature reaches a pre-determined set point (typically ~130 °C), the power supplied to the heater rods is automatically decreased or tripped. The R134a CHF test matrix along with the equivalent water pressure conditions used in the present experiments are

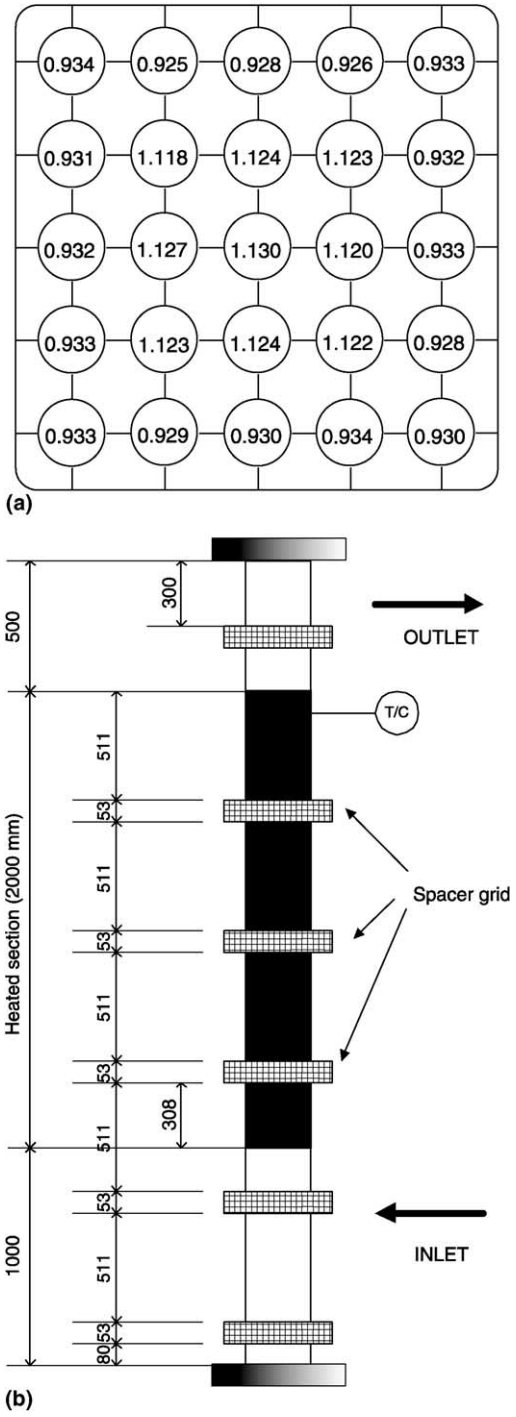

Fig. 2. (a) Normalized radial power distribution and (b) spacer grid locations.

given in Table 2. Based on the Manufacturer's specification and calibration procedures, the estimated errors in the measurement of the temperature, pressure and mass flux were ±0.5 °C, ±0.6% and ±0.1%, respectively. The maximum uncertainties for the CHF and critical quality are estimated as ±1.2% and ±0.04, respectively. The heat balance test showed that the heat loss is less than 1.9% of the total power applied to the test section.

Table 2
Conditions for the R134a CHF experiments

Pressure (MPa)		Inlet subcooling enthalpy (kJ kg^{-1})				
R134a	Water-equivalent					
1.50	9.2	10	25	–	–	–
1.97	11.8	10	25	40	–	–
2.47	14.5	10	25	40	55	–
2.97	17.0	10	25	40	55	70
R134a mass flux (kg m^{-2} s^{-1})		50, 150, 250, 350, 550, 750, 1000, 1500, 2000 and 2500				

3. Modeling methodology

In general, three basic similarities are required for a fluid-to-fluid modeling [1,2], namely

$$\text{Geometric similarity:} \quad \left(\frac{L}{D}\right)_{\mathrm{W}} = \left(\frac{L}{D}\right)_{\mathrm{F}}, \tag{1}$$

$$\text{Thermodynamic similarity:} \quad \left(\frac{\Delta h_{\mathrm{in}}}{h_{\mathrm{fg}}}\right)_{\mathrm{W}} = \left(\frac{\Delta h_{\mathrm{in}}}{h_{\mathrm{fg}}}\right)_{\mathrm{F}}, \tag{2}$$

$$\text{Hydrodynamic similarity:} \quad \left(\frac{\rho_{\mathrm{l}}}{\rho_{\mathrm{v}}}\right)_{\mathrm{W}} = \left(\frac{\rho_{\mathrm{l}}}{\rho_{\mathrm{v}}}\right)_{\mathrm{F}}, \tag{3}$$

where the subscripts 'W' and 'F' indicate the values for the water and the modeling fluid, respectively.

For modeling the mass flux, Ahmad [1], based on his dimensional analysis, recommended the following empirical compensated distortion parameter

$$\psi_{\mathrm{Ahmad}} = \left(\frac{GD}{\mu_{\mathrm{l}}}\right)\left(\frac{\mu_{\mathrm{l}}^2}{\sigma D \rho_{\mathrm{l}}}\right)^{2/3}\left(\frac{\mu_{\mathrm{v}}}{\mu_{\mathrm{l}}}\right)^{1/5}. \tag{4}$$

However, in most recent studies, the Katto's modeling parameter [2], recommended by Groeneveld et al. [3] has been adopted, which is

$$\psi_{\mathrm{Katto}} = \frac{G\sqrt{D}}{\sqrt{\sigma \rho_{\mathrm{l}}}}. \tag{5}$$

Once all the above similarities are satisfied, then the dimensionless CHF is expressed as

$$\frac{q''_{\mathrm{CHF}}}{Gh_{\mathrm{fg}}} = f\left(\psi, \frac{\Delta h_{\mathrm{in}}}{h_{\mathrm{fg}}}, \frac{\rho_{\mathrm{l}}}{\rho_{\mathrm{v}}}, \frac{L}{D}\right)_{\mathrm{F}}. \tag{6}$$

So that

$$(q''_{\mathrm{CHF}})_{\mathrm{W}} = \left(\frac{q''_{\mathrm{CHF}}}{Gh_{\mathrm{fg}}}\right)_{\mathrm{F}} (Gh_{\mathrm{fg}})_{\mathrm{W}}. \tag{7}$$

Note that the condition for a thermodynamic similarity Eq. (2) is based on the inlet condition whereas the CHF, in the case of the local condition approach, the thermodynamic similarity is expressed by equating the local qualities of the two fluids along any axial location of the heated length, i.e.,

$$(X(z))_{\mathrm{W}} = (X(z))_{\mathrm{F}}. \tag{8}$$

For heater rods with a uniform axial heat flux profile, the CHF always occurs at the exit of the heated section. For

this case, the critical quality, X_c, can be expressed by the following the heat balance equation:

$$X_c = \left(\frac{Q_c}{GA_f h_{fg}}\right) - \left(\frac{\Delta h_{in}}{h_{fg}}\right) \quad (9)$$

and Eq. (6) is rewritten as

$$\frac{q''_{CHF}}{Gh_{fg}} = f\left(\psi_{CHF}, Xc, \frac{\rho_l}{\rho_v}, \frac{L}{D}\right). \quad (10)$$

All the results and the modeling calculations to be discussed in subsequent sections are based on the rod bundle averaged CHF and the cross-sectional average conditions (i.e., using average hydraulic diameter, D_{hy}, cross-sectional averaged quality, X), as adopted in most experimental studies.

4. Results and discussion

4.1. R134a CHF results: parametric trends

Fig. 3 shows the effect of various parameters on the CHF. As shown in Fig. 3(a), for a given pressure and inlet subcooling, the effect of an increase in the mass flux is always to increase the CHF. At low mass fluxes ($G < 500\ \mathrm{kg\,m^{-2}\,s^{-1}}$), a CHF rapidly increases with an increase of the mass flux. However, the increasing trend of a CHF with the mass flux becomes almost linear for $G \geqslant 500\ \mathrm{kg\,m^{-2}\,s^{-1}}$. The slope of the increasing trend also becomes higher with an increase of the inlet subcooling. Fig. 3(b) shows that the effect of the inlet subcooling on the CHF is negligible at the lowest mass flux ($G = 50\ \mathrm{kg\,m^{-2}\,s^{-1}}$) considered, however, there exists an increasing trend for the CHF with the inlet subcooling which becomes increasingly prominent for the higher mass fluxes. This is also similar to that reported in previous works for simple geometries [11]. As shown in Fig. 3(c), the effect of an increasing pressure is to decrease the CHF in the present data. This trend should be expected since it is similar to the decreasing trend existing in the latent heat of vaporization with the pressure. The slope of the CHF decreasing trend with the pressure increases with an increasing mass flux which is similar in trend to that observed by Moon et al. [12] for a similar pressure range. However, for the highest mass flux considered

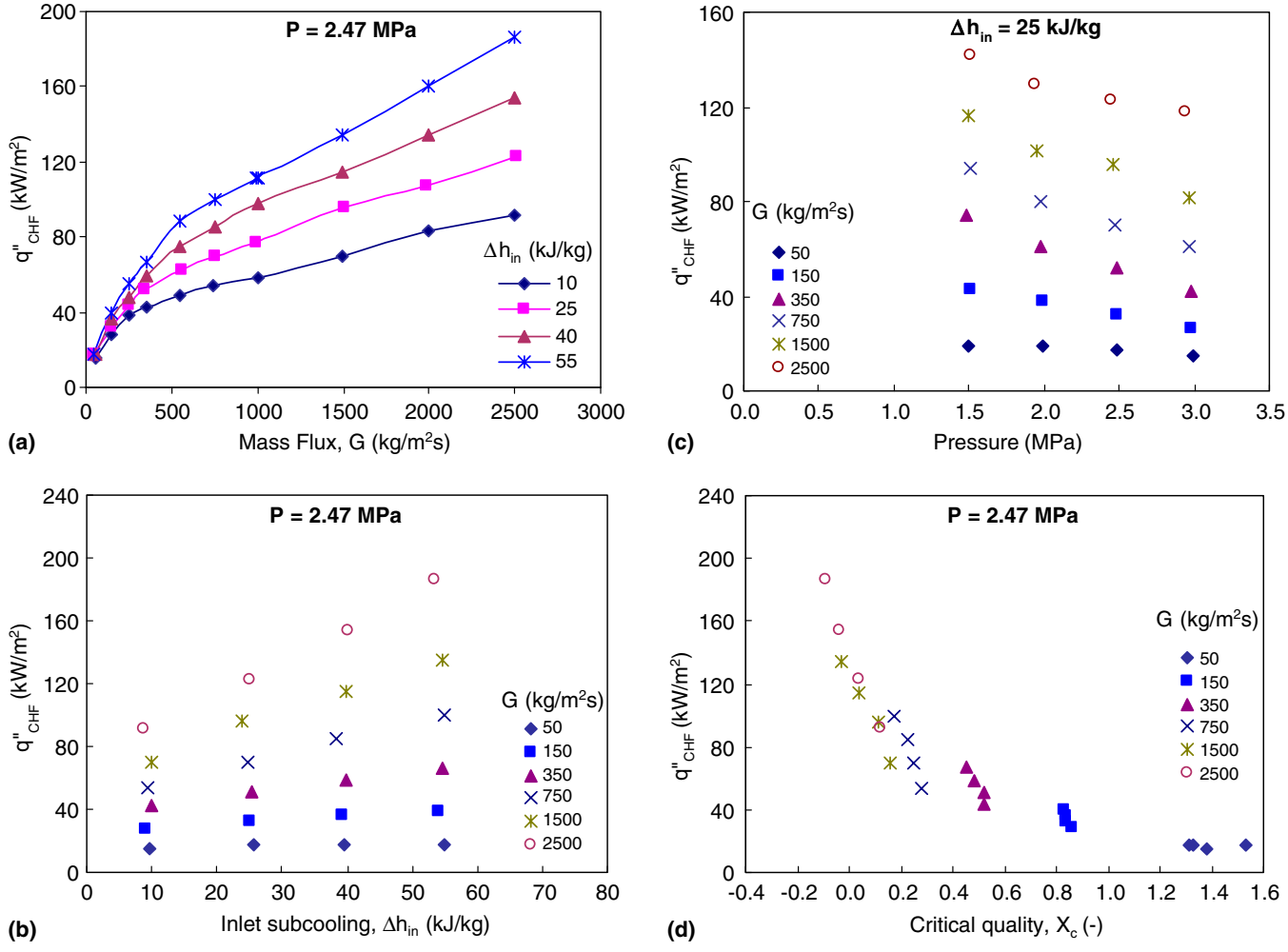

Fig. 3. Effect of various parameters on the CHF: (a) effect of the mass flux; (b) effect of the inlet subcooling; (c) effect of the pressure and (d) effect of the critical quality on a CHF.

($G = 2500\ \mathrm{kg\,m^{-2}\,s^{-1}}$), the effect of the pressure on the CHF begins to reduce at higher pressures. The reduced or negligible effect of the pressure on the CHF at higher mass fluxes ($G > 3000\ \mathrm{kg\,m^{-2}\,s^{-1}}$) has also been reported in previous studies [10]. Fig. 3(d) shows that only a small increase of the critical quality results in a sharp decrease of the CHF. The slope of the decreasing trend of a CHF with the critical quality is decreased for lower mass fluxes. This is similar to that reported by Moon et al. [12] and Kim and Chang [11]. No effect of the critical quality on a CHF is observed for the lowest mass flux ($G = 50\ \mathrm{kg\,m^{-2}\,s^{-1}}$) considered. This may be due to the fact that at very low flow conditions, a CHF is most likely caused by the countercurrent flow limitations (CCFL) wherein the dryout or depletion rate of the falling annular liquid film is restricted by the upward vapor flow in a subchannel. The critical quality at the lowest mass flux ($G = 50\ \mathrm{kg\,m^{-2}\,s^{-1}}$) is always observed to be greater than 1 ($X_c \sim 1.3$) in the present data. This proves the existence of a somewhat CCFL situation. Similar observations have been reported in previous experimental [12] and analytical [13] studies for CHF at zero or low flow conditions.

4.2. Comparison with EPRI/Columbia University's data

In order to assess the validity of the fluid-to-fluid modeling method for the present 5×5 rod bundle CHF data, a set of water CHF data with a uniform axial heat flux is chosen from the EPRI/Columbia University's database (hereafter CU data) [9] for the nearest (5×5 and 6×6) geometry and (water-equivalent) experimental conditions. The geometry parameters involved in the selected dataset are given in Table 3. For comparing the present water-equivalent results with the selected CU database involving different mass flux conditions, a dimensionless heat flux $q''_{\mathrm{CHF}}/Gh_{\mathrm{fg}}$ (Boiling number) versus Katto's parameter ψ_{Katto} and Ahmad's parameter ψ_{Ahmad} have been adopted. Water-equivalent pressures in the present data are 9.2, 11.8, 14.5 and 17.0 MPa, using the hydrodynamic similarity of Eq. (3). Whereas, the maximum CU's data is available at around 9.6, 12.2, 14.5 and 16.6 MPa pressures. Thus, in order to create a more realistic comparison between the present water-equivalent data and the CU data, the following procedure is adopted:

(i) The present data are converted by an interpolation to the nearest corresponding CU data pressure conditions.
(ii) Since, the dimensionless modeling parameters for a mass flux (Eqs. (4), and (5)) and the Boiling number (Eq. 6) are also the bases of the modeling methodology used, their values would be the same for both the R134a and the water-equivalent conditions in the present CHF data.
(iii) No CU data points are available at similar experimental conditions which exist in the present water-equivalent results. Thus, the CU data points, randomly existing within a ± 0.2 MPa pressure and ± 0.02 inlet quality, corresponding to the reference condition, have been considered for the comparison. Though, this methodology may cause a certain error (upto $\pm 5\%$), it was inevitably necessary to include the maximum possible CU datapoints for a comparison at a given pressure and inlet subcooling condition.
(iv) The comparison between the present and CU data is based on the cross-sectional average CHF conditions only.
(v) There exist some differences in the spacer grids types and locations used in the CU data tests relative to that in the present experiments, which are in turn likely to cause different effects, in the magnitude, on the CHF. However, due to the lack of necessary information, the effect of some differences in the spacer grids configurations on the cross-sectional average CHF has also been ignored. Both the present CHF data and CU data have uniform axial heat flux and simple plain grids without mixing vanes. Therefore, the effect of the spacer grids on the CHF may not be large enough to affect the comparison results between the present R134a CHF data and CU data.

For a rod bundle, it is very difficult to quantitatively estimate reliable local conditions, particularly at high quality and low flow conditions. Thus, the cross-sectional average CHF approach is adopted in the present study, as adopted in most of previous studies for a rod bundle. This can be supported by the fact that it is not always necessary for a CHF to occur in a subchannel involving the rod with the highest radial peaking factor. As observed in the pres-

Table 3
Geometry parameters of the test sections in CU's [9] water CHF experiments for rod bundles

Source of experiment	Test Sr. no.	Bundle geometry	Rod pitch (mm)	Rod diameter (mm)	Corner radius (mm)	Rod-to-wall gap (mm)	Heated length, L (mm)	Avgerage hydraulic diameter, D_{hy} (mm)	L/D_{hy} (–)	Radial power factor (–)
EPRI/CU	48	5×5	12.85	9.70	5.08	3.12	2134	10.43	205	1.025
EPRI/CU	62	5×5	12.85	9.70	5.08	3.12	2134	10.43	205	1.211
EPRI/CU	157	5×5	12.60	9.50	0.00	2.49	2438	9.69	252	1.111
EPRI/CU	160	5×5	12.60	9.50	0.00	2.49	2438	9.69	252	1.111
EPRI/CU	163	5×5	12.60	9.50	0.00	2.49	2438	9.69	252	1.111
EPRI/CU	411	6×6	12.73	9.63	0.00	4.57	1829	11.76	156	1.166
EPRI/CU	411.1	6×6	12.73	9.63	0.00	4.57	1829	11.76	156	1.166
Present		5×5	12.85	9.50	3.00	3.00	2000	10.69	187	1.130

ent experiments that, at low mass fluxes, a CHF is more likely to occur at the side rods, having radial peaking factors at about 20% less than those at the central region. Also, for a given test condition, a CHF is mostly recorded at more than one location simultaneously which makes it an impossible task to determine the actual location of the first CHF occurrence. Very similar trends are observed in the CU data [9]. Due to the mentioned reasons, though some differences in the maximum radial power factors exist within the CU data (up to 11%, see Table 3) relative to that in the present data, they are also not considered in the present comparisons.

Fig. 4 shows the comparison of the present dimensionless CHF (Boiling number, Bo) results with those for the CU data using Katto's modeling parameter, ψ_{Katto}. The results presented here are for the subcooling conditions involving a maximum number of CU's water CHF datapoints for each of the pressure cases. Except for the low values of the dimensionless mass flux parameter ($\psi_{\text{Katto}} < 100$) at the highest pressure of 16.6 MPa, the difference between the dimensionless heat fluxes of the present and CU databases is generally found to be within ±15%. For a pressure less than 14.5 MPa, a good agreement between the present and CU data is observed even for $\psi_{\text{Katto}} < 100$. Some scatter also exists within the CU data itself. So, keeping in view all the error sources including a possible error caused by some differences in the geometry condition, the validity of the fluid-to-fluid modeling methodology for the present rod bundle CHF data can be termed as reasonably good for the medium and high mass flux regions. For $\psi_{\text{Katto}} < 100$, however, considerable deviations (up to 25%) exist between the CU (water) and the present R134a (or water-equivalent) results for the highest pressure (16.6 MPa) which are similar to those observed by Chun et al. [10] for an annulus.

Fig. 5 shows a comparison of the present dimensionless CHF (Boiling number) results with the CU data using Ahmad's modeling parameter, ψ_{Ahmad} for the same parametric conditions. Except for the low values of the dimensionless mass flux parameter ($\psi_{\text{Ahmad}} < 6$) at the highest (16.6 MPa) pressure, the difference between the dimensionless heat fluxes of the present and CU databases is generally found to be within ±15% for all the cases. For the lower values of Ahmad's parameter ($\psi_{\text{Ahmad}} < 6$) at

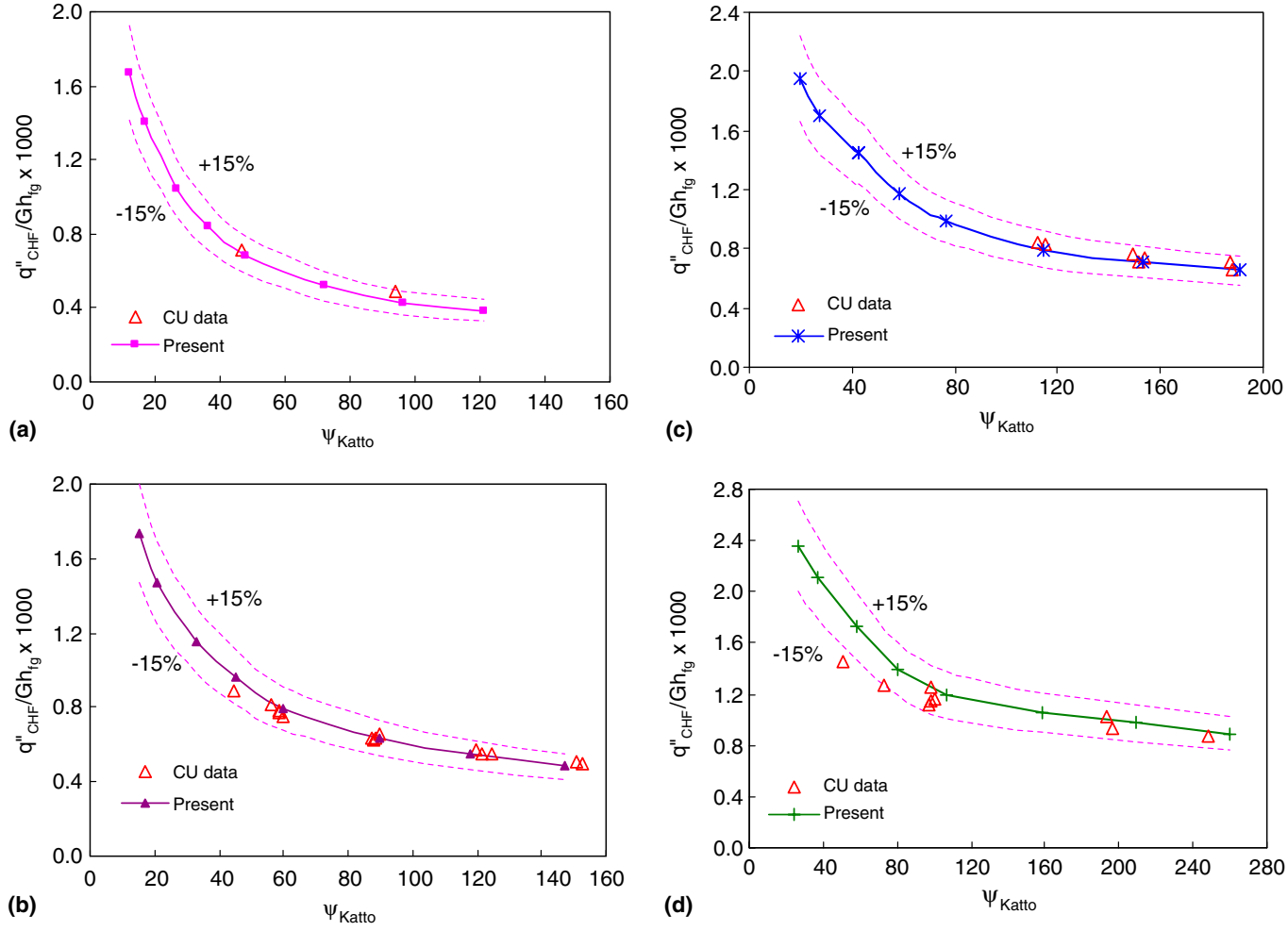

Fig. 4. Comparison with the CU data using Katto's parameter: (a) $P = 9.6$ MPa, $X_{\text{in}} = -0.18$; (b) $P = 12.2$ MPa, $X_{\text{in}} = -0.31$; (c) $P = 14.5$ MPa, $X_{\text{in}} = -0.49$ and (d) $P = 16.6$ MPa, $X_{\text{in}} = -0.75$.

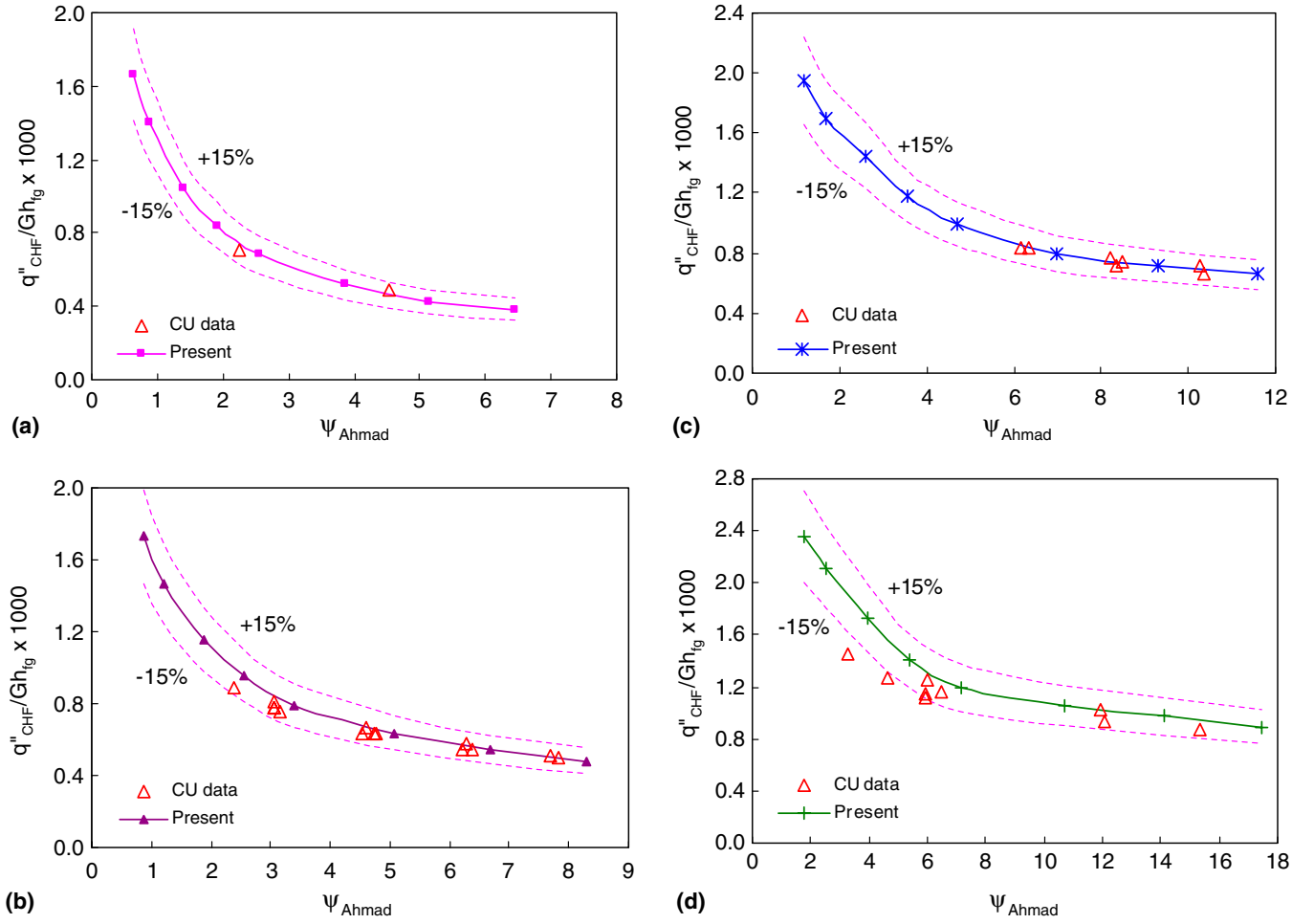

Fig. 5. Comparison with the CU data using Ahmad's parameter: (a) $P = 9.6$ MPa, $X_{in} = -0.18$; (b) $P = 12.2$ MPa, $X_{in} = -0.31$; (c) $P = 14.5$ MPa, $X_{in} = -0.49$ and (d) $P = 16.6$ MPa, $X_{in} = -0.75$.

16.6 MPa pressure, considerable deviations (up to 30%) exist between the CU (water) and the present R134a (or water-equivalent) results. The magnitudes of the deviations between the dimensionless CHFs of the present and the CU data are very similar for both Katto and Ahmad's parameters.

The possible cause for the considerable deviations at the low values of the modeling parameters (i.e., low mass fluxes) may be that, at equivalent conditions, the ratio of the frictional pressure drop to the system pressure in R134a is considerably (~15 times) higher than that in water [6,8]. This significant pressure drop causing the reduction in the saturation temperature of the modeling fluid may result in dissimilarity in the critical quality between water and R134a. According to Tain et al. [6], the difference in the axial quality gradients between water and the modeling fluid can also cause a dissimilarity of the phase (void fraction) distribution in both systems and thus limit the validity of the fluid-to-fluid to subcooled and low quality conditions only. Another reason for the deviation in the bundle case might be the bundle-specific effects, particularly the difference of the inter-channel mixing behavior between the water and Freon at the low flow conditions. However, further investigations are required to quantitatively estimate these effects.

Fig. 6 shows the overall results for the ratios of the Boiling numbers for the present-to-CU data ($Bo_{Pres}/Bo_{CU\,data}$) versus Katto and Ahmad's parameters. Except for the lower values of Katto's and Ahmad's parameters, the RMS deviations between the present and CU data are found to be only 7.0% and 5.1%, respectively (see Table 4).

4.3. Comparison with existing CHF correlations

It seems also useful to compare the present modeling results with some commonly used bundle-CHF prediction methods. For this purpose, the 1995 CHF look-up (LU) table method [14] along with the bundle-correction factors [14,15], the Bowring correlation [16] and the EPRI correlation [9] have been adopted by utilizing the heat balance method approach [17]. Fig. 7 shows the predicted CHF values in a comparison with the present (water-equivalent) CHF data. The largest deviations between the measured and predicted values were noted at the lowest mass flux

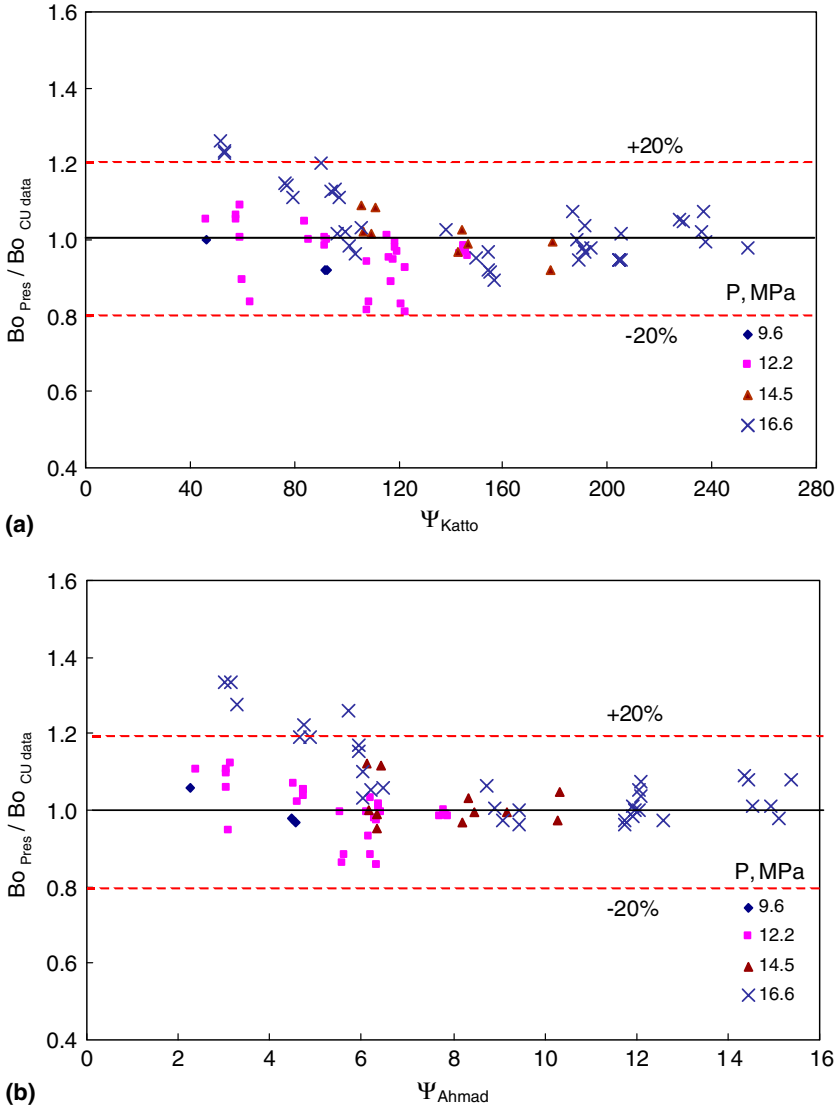

Fig. 6. Ratio of the Boiling numbers for the present-to-CU data versus modeling parameters: (a) Katto's parameter and (b) Ahmad's parameter.

Table 4
Estimated mean and RMS deviations between the present and CU data

Modeling parameter	Mean error (%)	RMS error (%)
Katto		
$\psi_{\text{Katto}} > 100$	−2.8	7.0
$\psi_{\text{Katto}} \leqslant 100$	6.6	11.8
Overall	3.0	8.9
Ahmad		
$\psi_{\text{Ahmad}} > 6$	0.8	5.1
$\psi_{\text{Ahmad}} \leqslant 6$	9.8	15.7
Overall	3.0	10.1

Note: Error $= \frac{\text{Value}_{\text{pred}} - \text{Value}_{\text{meas}}}{\text{Value}_{\text{meas}}}$, Mean error (%) $= \frac{100}{n}\sum_{i=1}^{i=n}\text{Error}_i$.

RMS error (%) $= \sqrt{\frac{1}{n}\sum_{i=1}^{i=n}\text{Error}_i^2} \times 100$.

($G_{\text{W}} \sim 70\ \text{kg m}^{-2}\ \text{s}^{-1}$) of water for all the prediction methods considered.

As an example, Fig. 8 shows the variation in the ratio of the predicted CHF to the measured CHF with the mass flux for the 1995 look-up table. This shows a significant (about 20–40%) under prediction at the lowest mass flux condition ($G_{\text{W}} \sim 70\ \text{kg m}^{-2}\ \text{s}^{-1}$). The main reason for such relatively large deviations may be that the conditions of a very low mass flux and a high local quality ($X_{\text{c}} > 1$) are not covered by the CHF prediction methods considered. Due to this reason, conditions of the lowest mass flux are not included while estimating the errors involved in the CHF prediction methods. The overall mean and RMS errors of the 1995 look-up table are only 2.0% and 10.4%, respectively, which are considerably less than those (mean error = 13.7%, RMS error = 17.4%) reported by Fortini and Veloso [18] for the 1995 look-up table in a comparison with the EPRI/CU's water CHF database for similar 25-rod bundles. Furthermore, an RMS error of about 8.0% also exists within the 1995 look-up table itself [19]. Thus, the agreement between the 1995 look-up table and the present (water-equivalent) results is good except very low flow conditions. Bowring correlations generally

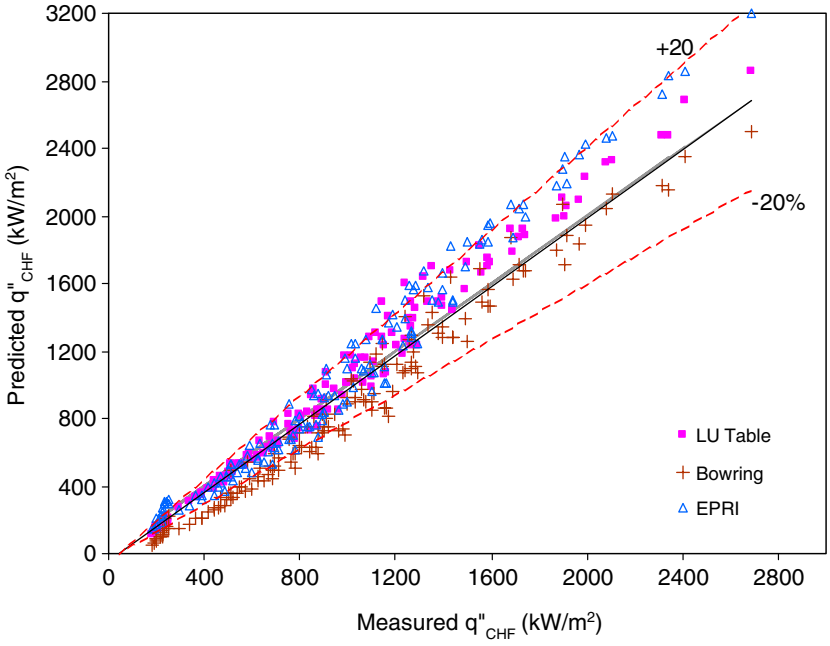

Fig. 7. Comparison of the predicted CHF with measured CHF.

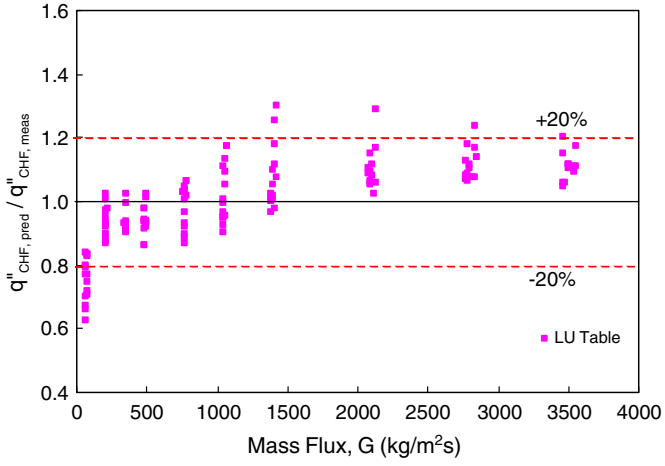

Fig. 8. Ratio of the measured-to-predicted CHF versus mass flux for the 1995 CHF look-up table.

gave significantly under-predicted CHF values when compared to the measured CHF values. The mean and RMS errors involved in the Bowring correlation predictions were −16.6% and 22.7%, respectively. Whereas, the EPRI correlation resulted in mean and RMS errors of 3.5% and 14.4%, respectively, which indicates a fairly good agreement with the measured results.

5. Conclusions

Fluid-to-fluid modeling principles have been assessed for the CHF of water in a uniformly heated rod bundle geometry. CHF tests were performed for a vertically upward R134a in the 5×5 rod bundle. Parametric trends of the measured R134a data have been analyzed and the water-equivalent data has been compared with the actual water CHF data as well as with the typical bundle-CHF prediction methods for water. The conclusions drawn are

(1) The measured CHF data of R134a shows parametric trends for the mass flux, pressure, inlet subcooling and local quality that are consistent with previous understandings. Negligible dependency of the CHF on the inlet subcooling and pressure at very low mass fluxes (i.e., $G = 50\ \mathrm{kg\ m^{-2}\ s^{-1}}$) is also consistent with previous works.

(2) In general, the water-equivalent CHF data generated from the present tests using both Katto's and Ahmad's modeling methods agree reasonably well with the CU data for similar geometries. Except for the low flow conditions ($\psi_{\mathrm{Katto}} < 100$ and $\psi_{\mathrm{Ahmad}} < 6$), the RMS deviations between the present and CU data results are 7.0% and 5.1% for Katto's and Ahmad's modeling methods, respectively.

(3) The generated water-equivalent CHFs are also predicted reasonably well by the 1995 CHF look-up table and the EPRI correlation while the Bowring correlation gave an under prediction. The 1995 look-up table method, involving mean and RMS errors of 2.0% and 10.4%, respectively, is found to be the best-fit prediction method with the present results.

(4) Considering the present investigation and the previous works, the R134a is assessed to be a good modeling fluid for the CHF of a high-pressure water except for the very low flow conditions.

Acknowledgements

This work was performed as a part of the Long-term Nuclear Energy R&D Program which was financially supported by the Ministry of Science and Technology of Korea. The authors also like to thank Regional Co-operative Agreement (RCA) Regional Office, Korea, for facilitating the participation of Dr. S.W. Akhtar in this project under the RCA Post-doctoral Fellowship Programme.

References

[1] S.Y. Ahmad, Fluid to fluid modeling of CHF: A compensated distortion model, Int. J. Heat Mass Transfer 16 (1973) 641–662.
[2] Y. Katto, A generalized correlation of CHF for the forced convective boiling in vertical uniformly heated round tubes, Int. J. Heat Mass Transfer 21 (1978) 1527–1542.
[3] D.C. Groeneveld, B.P. Kiameh, S.C. Cheng, Prediction of critical heat flux (CHF) for non aqueous fluids in forced convective boiling, in: Proc. 8th Int. Heat Transfer Conf., San Francisco, California, USA, vol. 5, 1986, pp. 2209–2214.
[4] S.S. Doerffer, D.C. Groeneveld, R. Tain, S.C. Cheng, W. Zeggel, Fluid-to-fluid modeling of the CHF in simple and complex geometries, AECL Report ARD-TD-321, Atomic Energy of Canada Limited, Chalk River, Canada, 1991.
[5] I.L. Pioro, D.C. Groeneveld, S.C. Cheng, S. Doerffer, A.Z. Vasic, Y.V. Antoshko, Comparison of CHF measurements in R134a cooled tubes and the water CHF look-up table, Int. J. Heat Mass Transfer 44 (2001) 73–88.
[6] R.M. Tain, D.C. Groeneveld, S.C. Cheng, Limitations of the fluid-to-fluid scaling technique for CHF in flow boiling, Int. J. Heat Mass Transfer 38 (12) (1995) 2195–2208.
[7] I.L. Pioro, S.C. Cheng, A.Z. Vasic, R. Felisari, Some problems for bundle CHF prediction based on CHF measurements in simple flow geometries, Nucl. Eng. Design 201 (2000) 189–207.
[8] A. Katsaounis, Verification of Ahmad's fluid-to-fluid scaling law by bundle experiments, in: Proc. Winter Annual Meeting of the ASME, Chicago, USA, 1980, pp. 37–44.
[9] C.F. Fighetti, D.G. Reddy, Parametric study of CHF data, EPRI Report NP-2609, Electric Power Research Institute, Palo Alto, California, USA, 1982.
[10] S.Y. Chun, S.D. Hong, Y.S. Cho, W.P. Baek, Comparison of the CHF data for water and refrigerant HFC-134a by using the fluid-to-fluid modeling methods, Int. J. Heat Mass Transfer, in press, doi:10.1016/j.ijheatmasstransfer.2005.06.039.
[11] C.H. Kim, S.H. Chang, CHF characteristics of R134a flowing upward in uniformly heated tube, Int. J. Heat Mass Transfer 48 (11) (2005) 2242–2249.
[12] S.K. Moon, S.Y. Chun, S. Cho, W.P. Baek, An experimental study on the critical heat flux for low flow of water in a non-uniformly heated vertical rod bundle over a wide range of pressure conditions, Nucl. Eng. Des. 235 (2005) 2295–2309.
[13] C. Park, W.P. Baek, S.H. Chang, An improved physical model for flooding limited CHF under zero and very low flow conditions, Int. Commun. Heat Mass Transfer 25 (3) (1998) 339–348.
[14] D.C. Groeneveld, L.K.H. Leung, P.L. Kirillov, V.P. Bobkov, I.P. Smogalev, V.N. Vinogradov, X.C. Huang, E. Royer, The 1995 look-up table for critical heat flux in tubes, Nucl. Eng. Des. 163 (1996) 1–23.
[15] M. Lee, A CHF approach for square rod bundles using the 1995 Groeneveld CHF table and bundle data of heat transfer facility, Nucl. Eng. Des. 197 (2000) 357–374.
[16] R.W. Bowring, WSC-2: Subchannel Dryout Correlation for Water-Cooled Cluster Over Pressure Range 3.4–15.9 MPa, AEEW-R983, United Kingdom Atomic Energy Agency, Winfrith, 1979.
[17] M.S. Tov, Application of energy balance and direct substitution methods for thermal margins and data evaluation, Nucl. Eng. Des. 163 (1996) 249–258.
[18] M.A. Fortini, M.A. Veloso, CHF prediction in nuclear fuel elements by using round tube data, Ann. Nucl. Energy 29 (2002) 2071–2085.
[19] W.P. Baek, H.C. Kim, S.H. Chang, An independent assessment of Groeneveld et al.'s 1995 CHF lookup table, Nucl. Eng. Des. 178 (1997) 331–337.